한국기계가공학회지, 제19권, 제12호, pp. 1~7(2020.12) ISSN 1598-6721(Print)
Journal of the Korean Society of Manufacturing Process Engineers, Vol. 19, No. 12, pp. 1~7(2020.12)ISSN 2288-0771(Online)

https://doi.org/10.14775/ksmpe.2020.19.12.001

Evaluation of Bending Fatigue Testing of Austempered Ductile Iron Spur Gears

Jian Hua Lv[*], Rui Zhou[*], Yang Xu[**], Zhen Qin[***], Qi Zhang[*,#1], Sungki Lyu[***,#2]

[*]R&D Department, Zhejiang Shuanghuan Driveline Co., LTD., China
[**]School of Material Science and Engineering, Xi' an University of Technology, China
[***]School of Mechanical & Aerospace Engineering, Gyeongsang National University, Korea

오스템퍼링 구상흑연주철 평기어의 굽힘피로시험평가에 관한 연구

려건화*, 주서*, 허양**, 진진***, 장기*,#1, 류성기***,#2

*중국 절강쌍환전동유한회사, **중국 서안이공대학 재료공학부, ***경상대학교 대학원 기계항공공학부

(Received 11 August 2020; received in revised form 30 September 2020; accepted 03 October 2020)

ABSTRACT

An experimental evaluation of bending fatigue strength for austempered ductile iron (ADI) spur gears was performed using a Zwick fatigue tester. The gear material was manufactured using vertical continuous casting, resulting in the radius of the graphite grains being smaller. The stress–number of cycles curve (S–N curve) for the bending fatigue strength of the ADI spur gears thus manufactured, without any specific surface treatments, was obtained using post-processing software. It was observed that when the reliability was 50%, the allowable root stress was 610 MPa. was calculated using an analytical method as well as the finite element method, and the difference between the values calculated using the two methods is only 7%. This study provides a reliable basis to rate the reliability design of small gearboxes in automation in the future.

Keywords : Vertically Continuous Casting(세로 연속주조법), ADI(오스템퍼링 구상흑연 주철), Gear(기어), Bending Fatigue (굽힘피로)

1. Introduction

Ductile iron materials have been known to have excellent machinability. However, as they have been mistakenly supposed to be brittle, people often overlook them when selecting engineering materials. Ductile iron is composed of steel as a matrix, to which graphite is added. It contains more Si, Mn, and other elements than steel does; these elements dissolve in the metal matrix and strengthen it. In addition, the graphite of ductile iron exists in the form of spheres, so that the splitting effect of graphite on the matrix is relatively small, which significantly improves the mechanical properties and

#1 Corresponding Author : zhangqi@gearsnet.com
Tel: +86-576-8723-9883, Fax: +86-576-8723-9827
#2 Corresponding Author : sklyu@gnu.ac.kr
Tel: +82-55-772-1632, Fax: +82-55-772-1578

processing properties of ductile iron. Its performance can also be improved by changing its composition and structure through alloying and heat treatment processes, such as austempering. Consequently, the strength and hardness of austempered ductile iron (ADI) are higher than those of steel.

In actual applications, ADI offers design engineers an alternative to conventional materials. Depending on the material and the application, austempering may provide many benefits to producers of powertrain components such as gears and shafts[1,2]. ADI has been used to create small gearboxes for automation[3,4], e.g. high precision planetary gearboxes. It may also potentially be used to create gear materials for other high precision reducers, such as RV cycloid and harmonic drives.

In the experiment conducted in this study, instead of horizontal continuous casting[5], vertical continuous casting was used to produce a solid cast-iron bar to use as the material of spur gears. Single tooth fatigue (STF) tests of ADI spur gears were performed using a Zwick fatigue tester, through which the gear loads were applied by loading an anvil in a single gear. In addition, the fatigue limit was obtained to rate the design for small gearboxes to be used in automation in the future.

2. Material and Test Gears

Based on the structure and application characteristics of the gears for small gearboxes in automation, the gear size should be relatively smaller, the wall thickness should be uniform, and the structure should be quite simple. Vertical continuous casting is used to produce a solid cast-iron bar, which is used to create the spur gear material for bending fatigue testing.

2.1 Vertical Continuous Casting

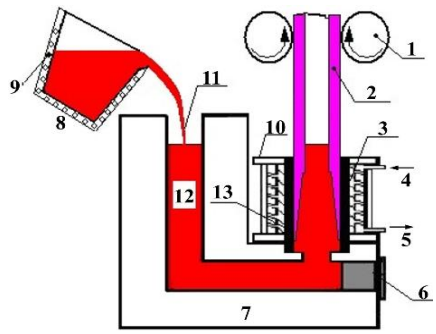

Fig. 1 Schematic of vertical continuous casting (1) Pulling roller, (2) Hollow profile, (3) Crystallizer, (4) Water intake, (5) Water outlet, (6) Liquid iron mouth, (7) Continuous casting furnace, (8) Teapot ladle, (9) Heater, (10) Upper flange, (11) Casting port, (12) Molten iron, (13) Graphite sleeve

Vertical continuous casting utilizes the principle of central solidification, as shown in Fig. 1. It also takes advantage of the time taken for the thickness of the solidified layer to gradually increase from thin to thick, increasing the thermal strength of the cast iron material and prevent any effect of gravity on the liquid level of the molten iron. The casting process of vertical continuous casting is very similar to that of horizontal continuous casting, but the eutectoid transformation during the vertical continuous casting process is not affected by the high temperature of the molten iron (liquid core). The cooling rate is faster and component segregation is effectively eliminated. The microstructure is more uniform and finer, while the spheroidization rate is higher. The radius of the graphite grains is smaller[6,7]. Consequently, the mechanical properties and the microstructures are superior to the bars produced by sand casting.

A key feature of hollow cast-iron produced using vertical continuous casting is that neither an inner core crystallizer nor a graphite inner core guided mold is used in the continuous casting of copper tubes and aluminum tubes[8]. The material is completely free to form by means of central

solidification of the molten iron. Therefore, there are strict requirements for the composition of molten iron and its pull-stop relationship.

2.2 Test Gears

In general, the main factors contributing to gear contact fatigue, scuffing, and bending fatigue are gear material (composition, quality, and heat treatment), design (macro-geometry and micro-geometry), manufacturing process (shaving, grinding, honing, surface roughness, and accuracy), surface treatment (shot-peening for compressive residual stress, superfinishing, and coating) and operating conditions (torque, speed, lubrication, temperature, and duty cycles).

In order to improve the quenching process and mechanical properties, certain amounts of alloy elements such as Cu, Mn, Mo, and Ni are added to produce suitable ADI material[9,10], mainly to improve the hardenability and prolong the stability of the structure and properties during isothermal quenching. The ADI gear material considered in this study is ausferritic spheroidal graphite cast iron produced by vertical continuous casting and austempering heat treatment process control. Table 1 presents the chemical composition of the material.

Based on previous studies, ADI gear fatigue strength is improved by the machining process of austempering after hobbing or surface treatments like shot-peening and fine particle bombarding[11–15]. The dimensions of the test spur gears used for the experiment, which are manufactured without specific surface treatments, are listed in Table 2. The material used for the test gear corresponds to GB QTD 1200-3[16]. The measured tensile stress was about 1200–1400 MPa. Table 3 lists the mechanical properties of the base material.

The steps in the manufacturing process of test gears are: vertical continuous casting, sawing, annealing, rough turning, finish turning, hobbing, austempering, and grinding. The accuracy of the test gears was ISO 6, the tooth surface roughness was Ra 0.8, and the radius of the generated tooth root fillet was approximately 0.93 mm.

Table 1 Chemical composition of the base material(wt%)

C	Si	Cu	Ni	Cr	Mn
3.23	2.75	0.63	0.55	0.16	0.13

Table 2 Dimensions of test gear

Description	Symbol	Unit	Value
Module	m	mm	2.5
Number of teeth	z	-	38
Pressure angle	α	deg.	20
Profile modification coefficient	x	-	0
Face width	b	mm	30
Pitch circle diameter	d	mm	89.271
Tip circle diameter	da	mm	100
Root circle diameter	df	mm	88.750

Table 3 Mechanical properties of the material

Description	Symbol	Unit	Value
Tensile strength	Rm	MPa	1400
Proof strength	RP0.2	MPa	1050
Elastic module	E	GPa	153
Poisson's ration	μ	-	0.25
Elongation	A	%	2
Density	ρ	g/㎤	7.06

Austempering involves heat treatment at 900°C for 1 hour and rapid quenching at 250°C in a salt bath for 1 hour. After completion of the heat treatment and the grinding machining, the tooth surface was etched in 4% nital and polished. The gear tooth microstructure contains uniform upper bainite and austenite. The microstructure of ADI is shown in Fig. 2. Hardness measurements are given in Fig. 3, which provides the measured hardness as a function of depth from the surface.

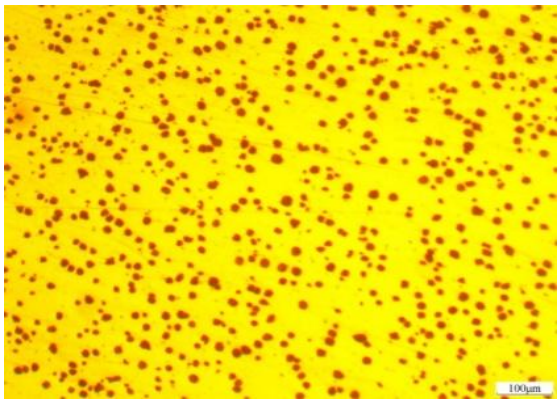

Fig. 2 Microstructure of ADI

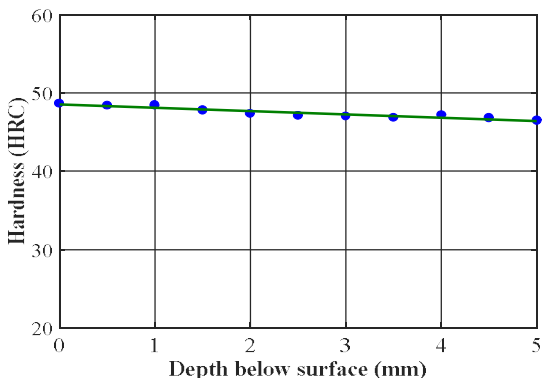

Fig. 3 Hardness distribution along with the depth

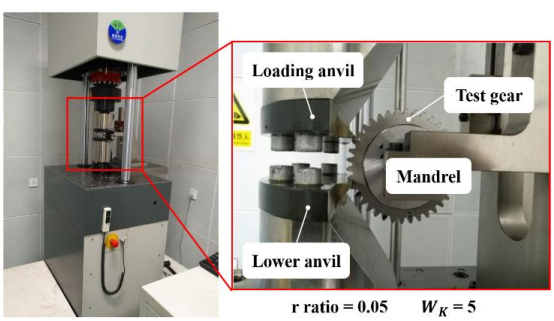

Fig. 4 Bending fatigue test rig

3. Bending Test

Based on differences in loading method, operation mode, and structural style of the gear fatigue test device, the gear fatigue test device is mainly divided into two forms. One form is a non-operating test, and the other is a running test. The former method can be efficiently applied to a single-parameter rapid comparative test to determine the influence of various loads, materials, tooth profiles, and other factors on the bending fatigue strength of gear teeth. The latter device is used to test the gear during operation, and can simulate the actual situation of the gear in its working condition, but at a higher cost.

STF fatigue tests were performed using a Zwick/Amsler 250 HFP 5100 fatigue tester in the pulsating loading mode. As shown in Fig. 4, the fatigue testing machine is equipped with a test fixture, and the fixture is specially designed in accordance with the standard requirements[17]. The operating frequency is about, the base tangent length spanned in gear teeth k is 5, and the stress ratio r is set as 0.05 to prevent the test teeth from separating from the load anvil during unloading.

The ISO strength rating standard recommends a life factor of unity at the life of N≥3×106 for heat-treated gears[17]. Thus, if the test tooth is not broken before N=3×106, the test is terminated and is considered to be a success. For the gear bending fatigue performance, in order to fully understand the relationship between the test load/stress and the tooth bending fatigue life of N, the group method and the staircase method are implemented to obtain the S–N curves. Six test loads and nine samples for each load are tested to determine the S–N curve.

4. Data Processing

Reasonable processing of the original data obtained from the experiment is the premise of fitting the S–N curve. The processing involves tooth root stress calculation, a correlation test of the original data, the fitting of the S–N curve under contract reliability, and similar steps.

4.1 Tooth Root Stress Calculation

The normal force is loaded on the gear during the test, and the root stress needs to be calculated as per the loaded force and the loaded position. This study uses the finite element method and the analytical method to calculate root stress.

4.1.1 Finite element method

The finite element method can determine the distribution of tooth root stress and the position of the dangerous section. It can also reduce the cost of the test to a certain extent. Based on the parameters in Table 2, a three-dimensional solid model of the gear is obtained and imported into an ANSYS workbench. The material parameters listed in Table 3 are uploaded into the software, and the resulting tooth root stress is given in Fig. 5. The result of the finite element calculation is the nominal tooth root stress σ_{F0}, which can be converted into allowable root stress σ_{FE}. The conversion method is given in Eq. (1). The results of the calculation are presented in Table 4.

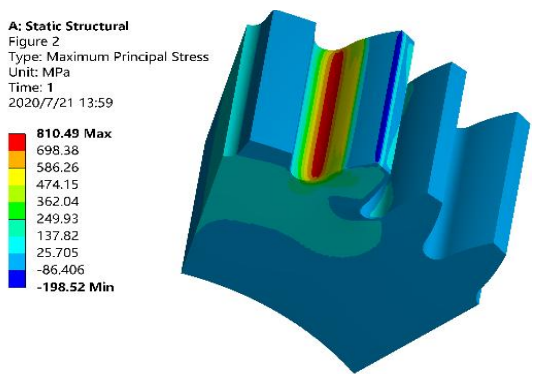

Fig. 5 Maximum principal stress

Table 4 The test loads and allowable root stress σ_{FE}

	I	II	III	IV	V	VI
Loads F (kN)	21	18.6	17.5	17	16.5	16
FEM σ_{FE} (MPa)	726	643	605	588	571	554
AM σ_{FE} (MPa)	780	692	648	632	612	592

4.1.2 Analytical method

The analytical method is performed according to ISO 6336. This standard considers the 30° tangent of the tooth root transition fillet to be the dangerous section[17-18], and formula (1) is used to calculate the tooth root stress.

$$\sigma'_F = \frac{\sigma_{F0}}{Y_{ST} Y_{\delta relT} Y_X} = \frac{\sigma_{FE}}{Y_{ST}} \quad (1)$$

in which,

σ'_F : tooth root stress,

σ_{F0} : nominal tooth root stress,

σ_{FE} : allowable root stress,

Y_{ST} : stress correction factor, YST=2.0,

$Y_{\delta relT}$: relative notch sensitivity factor,

Y_{RrelT}: relative surface factor,

Y_X : size factor

The above coefficients are obtained according to ISO 6336, and then σ'_F can be calculated, but σ'_F is the tooth root stress when the load factor r=0.05, which needs to be converted to the tooth root stress σ_F when r=0. See Eq. (2).

$$\sigma'_F = \frac{(1-r)\sigma'_F}{1-r\frac{\sigma'_F}{R_m+350}} \quad (2)$$

In Eq. (2), R_m is the tensile stress, as given in Table 3. Table 4 lists the test loads and the results of allowable root stress number σ_{FE} for the two calculation methods. Based on calculation and comparison, it can be seen that the difference between the results of the two methods is about 7%.

4.2 Correlation Test and Distribution

The statistical methods commonly used for gear bending fatigue test data are log-normal distribution and Weibull distribution[19]. The fatigue life and

Table 5 Correlation coefficient

Distribution type	Correlation coefficient r			
	21 kN	18.6 kN	17.5 kN	17.0 kN
Log normal	0.9635	0.9518	0.9673	0.9675
Weibull	0.9309	0.9038	0.9503	0.9371

failure probability data under each load level are linearly fitted using the least-squares method, and the correlation coefficients of the two distribution types are calculated, as presented in Table 5. By comparing the correlation coefficients of several probability distributions, it is found that the log-normal distribution best fits the given stress for the bending fatigue life with better flexibility and adaptability.

4.3 R-S-N Curves

After the above calculation, the S–N curve can be fitted. This was done using post-processing software SAFD 5 (Statistical Analysis of Fatigue Data)[20], as shown in Fig. 5, and the equation parameter of gear bending fatigue and the bending fatigue limit were obtained.

Fig. 6 shows the S–N curves for the bending fatigue strength of ADI spur gears. When the reliability is 95%, the bending fatigue limit of the ADI spur gear is 582 MPa. When the reliability is

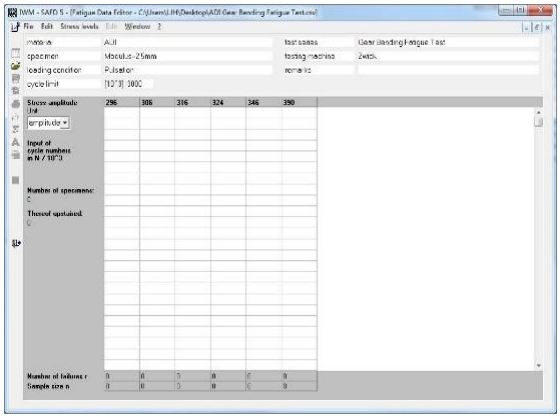

Fig. 5 SAFD data post-procession software

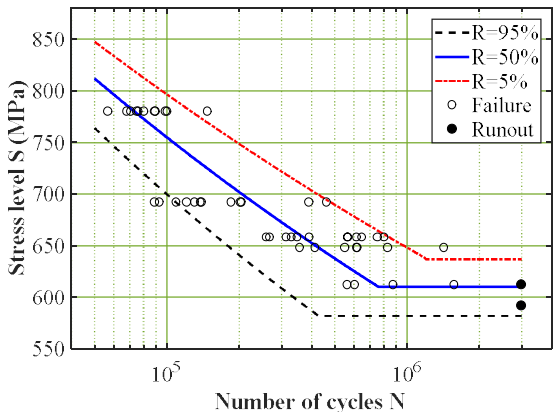

Fig. 6 ADI fatigue life and S-N curves

50%, the fatigue limit is 610 MPa. When the reliability is 5%, the fatigue limit is 638 MPa. The value of the nominal stress number (bending) σ_{FE} in Ref. 11 for ADI is about 576 MPa, which is used as a reference to evaluate the reasonability of the experiment.

4. Conclusions

In this study, the tooth root stress was calculated using the finite element method and the analytical method, and the difference between the two calculation results was only about 7%, which verified the accuracy of the finite element calculation result. The tooth root stress of the finite element method distribution diagram also illustrates the correctness of the analytical dangerous section.

STF fatigue tests were performed to study and analyze the bending fatigue strength of ADI spur gears, whose material was manufactured by vertical continuous casting. The S–N curves of ADI gear material for the bending fatigue strength were obtained using reliability theory. The results show that when the reliability is 50%, the fatigue limit is 610 MPa. The experiment also provides a reliable basis for the design of small gearboxes in automation.

Acknowledgements

This study was supported by the Basic Science Research Program through the NRF of Korea (NRF-2020R1A2C1011958) funded by the MEST. Many thanks are also due for the support from the Science Technology Department of Zhejiang Province.

References

1. Lefevre, J., Hayrynen, K. L., "Austempered Materials for Powertrain Applications," Journal of Materials Engineering and Performance, Vol. 22, No. 7, pp. 1914-1922, 2013.
2. Guesser, W. L. et al., "Austempered Ductile Iron for Gears," SAE Technical Paper 2012-36-0305, 2012.
3. Concli, F., "Austempered Ductile Iron (ADI) for gears: Contact and bending fatigue behavior," Procedia Structural Integrity, No. 8, pp. 14-23, 2018.
4. Gorla, C., Conrado, E., Rosa, F., and Concli, F., "Contact and bending fatigue behaviour of austempered ductile iron gears," Proc IMechE Part C: J Mechanical Engineering Science, Vol. 232, No. 6, pp. 998-1008, 2018.
5. Pongsak, C., Panya, S., Continuously cast ductile iron: Processing, structures, and properties. Journal of Materials Processing Technology, Vol. 211, No. 8, pp. 1372 - 1378, 2011.
6. Yan, G., Xu, Y., Jiang, B., "The Production of High-density Hollow Cast-iron Bars by Vertically Continuous Casting," Journal of Materials Processing Technology, Vol. 212, No. 1, pp. 15-18, 2012.
7. Xu, Y. et al., Casting Manual: Special Casting P rocess, 4th ed., China Machine Press, China. (accepted, in press)
8. Xu, Y., Deng, K., Jiang, B. et al., "Research on Growth Model of Solidified Layer in Continuous Cast Iron Hollow Profile," Foundry Technology, Vol. 36, No. 4, pp. 953-956, 2015.
9. Liu, S., Chen, Y. et al., "Microstructure and Mechanical Properties of Helical Bevel Gears Made by Mn-Cu Alloyed Austempered Ductile Iron," Journal of Iron and Steel Research, Vol. 19, No. 2, pp. 36-42, 2012.
10. Zammit, A., Abela, S. et al., "Tribological behaviour of shot peened Cu - Ni austempered ductile iron," Wear, Vol. 302, No. 1-2, pp. 829-836, 2013.
11. Yamanaka, M., Tamura, R., Inoue, K. Narita, Y., "Bending Fatigue Strength of Austempered Ductile Iron Spur Gears," Journal of Advanced Mechanical Design, Systems, and Manufacturing, Vol. 3, No. 3, pp. 203-211, 2009.
12. Inoue, K., Kato, M. et al., "Bending strength of spur gear teeth made of austempered ductile iron," Transactions of the Japan Society of Mechanical Engineers (Series C), Vol. 55, No. 512, pp. 999-1003, 1989.
13. Oda, S., Yano, M. et al., "Bending Fatigue Strength of Austempered Ductile Iron Gears," Transactions of the Japan Society of Mechanical Engineers (Series C), Vol. 56, No. 532, pp. 3416-3419, 1990.
14. Zammit, A., Mhaede, M. et al., "Influence of shot peening on the fatigue life of Cu - Ni austempered ductile iron," Materials Science and Engineering: A, No. 545, pp. 78-85, 2012.
15. Zammit, A., Bonnici, M. et al., "Shot peening of austempered ductile iron gears," Surface Engineering, Vol. 33, No. 9, pp. 679-686, 2017.
16. GB/T 24733, Austempered ductile iron (ADI) castings, 2009.
17. GB/T 14230-93, Standard of test method for bending load capacity of gears, 1993.
18. ISO6336, Calculation of load capacity of spur and helical gears, 2006.
19. Gao, Z., Xiong, J., "Fatigue reliability," Beijing University of Aeronautics and Astronautics Press, 2000.
20. SAFD Manual, version 5.5, Institute for Materials Applications in Mechanical Engineering, RWTH Aachen University, 2006.